HAL open science

Diurnal cycle of dust and cirrus over West Africa as seen from meteosat second generation satellite and a regional forecast model.

Jean-Pierre Chaboureau, Pierre Tulet, C. Mari

To cite this version:

Jean-Pierre Chaboureau, Pierre Tulet, C. Mari. Diurnal cycle of dust and cirrus over West Africa as seen from meteosat second generation satellite and a regional forecast model.. Geophysical Research Letters, 2007, 34, pp.L02822. 10.1029/2006GL027771 . hal-00130155

HAL Id: hal-00130155

https://hal.science/hal-00130155v1

Submitted on 20 Jul 2021

HAL is a multi-disciplinary open access archive for the deposit and dissemination of scientific research documents, whether they are published or not. The documents may come from teaching and research institutions in France or abroad, or from public or private research centers.

L'archive ouverte pluridisciplinaire **HAL**, est destinée au dépôt et à la diffusion de documents scientifiques de niveau recherche, publiés ou non, émanant des établissements d'enseignement et de recherche français ou étrangers, des laboratoires publics ou privés.

Copyright

Diurnal cycle of dust and cirrus over West Africa as seen from Meteosat Second Generation satellite and a regional forecast model

Jean-Pierre Chaboureau,[1] Pierre Tulet,[2] and Céline Mari[1]

Received 7 August 2006; revised 6 November 2006; accepted 29 December 2006; published 30 January 2007.

[1] A brightness temperature difference (BTD) technique is used to evaluate the dust and cirrus forecasts of a regional meteorological model. The technique based on a contrasted absorption property of dust and cirrus at two wavelengths within the atmospheric infrared window is applied to 3-hourly Meteosat Second Generation (MSG) observations in the 10.8- and 12-μm bands over West Africa. The satellite observation of dust coverage over the Sahara shows a well marked diurnal cycle associated with the boundary layer activity peaking at 15 UTC. A similar signature is obtained from the regional model when the dust scheme is activated. The cirrus cover over West Africa is maximum at 12 UTC as seen both from MSG and the model. The use of prognostic dust aerosol, instead of climatology, furthermore better captures the observed convective activity. **Citation:** Chaboureau, J.-P., P. Tulet, and C. Mari (2007), Diurnal cycle of dust and cirrus over West Africa as seen from Meteosat Second Generation satellite and a regional forecast model, *Geophys. Res. Lett.*, *34*, L02822, doi:10.1029/2006GL027771.

1. Introduction

[2] Mineral dust aerosols and cirrus play an important role in climate by altering the radiation budget. Their radiative direct effect can modify the general circulation on climate timescale, but also at shorter time scales. Recently, a revision of the aerosol climatology in the forecasting system at ECMWF has significantly improved the ECMWF 5-day forecasts of the African Easterly Jet (AEJ), the central dynamical feature over West Africa [*Tompkins et al.*, 2005]. To a large extent, dust and cirrus are products of surface and planetary boundary layer (PBL), and convective processes, respectively. Dominant dust sources in North Africa are natural dry topographic depressions [e.g., *Yoshioka et al.*, 2005] while half of the tropical cirrus are originated from deep convection [*Comstock and Jakob*, 2004]. Both dust and cirrus can be advected over large distances away from their sources. Thus their modeling requires prognostic equations with a subgrid-scale source and a transport term. This combination makes their representation difficult.

[3] Investigating the atmospheric diurnal cycle can be very useful to identify fundamental shortcomings in atmospheric modeling [e.g., *Bechtold et al.*, 2004]. Over North Africa, diurnal variability in dust mobilization can vary from 55 to 75% depending on model configurations [*Luo et al.*, 2004]. Over Brazil, the correct diurnal cycle of upper-tropospheric humidity is obtained after tuning a critical parameter in a cirrus parameterization constrained by MSG observations [*Chaboureau and Pinty*, 2006]. The later study adopted a model-to-satellite approach, in which satellite brightness temperature (BT) images are directly compared to BTs computed from predicted model fields [*Morcrette*, 1991]. This approach is especially powerful in identifying discrepancies of cloud cover forecasts [*Chaboureau et al.*, 2002]. The present paper shows how a split-window technique associated with the model-to-satellite approach can give an assessment of the dust and cirrus cover forecasts.

[4] The split-window technique is often used for retrieving microphysical properties of cirrus clouds [e.g., *Inoue*, 1985]. The technique is based on a contrasted absorption property of ice crystals at two channels located within the atmospheric infrared window. More specifically, positive brightness temperature difference (BTD) between the 10.8- and 12-μm bands are observed from thin ice clouds. On the other hand, negative BTD are observed from dust storms [*Ackerman*, 1997; *Sokolik*, 2002]. Furthermore, a method for detecting and differentiating dust from cirrus combining shortwave reflectance ratio tests with longwave BTD has also been developed [*Roskovensky and Liou*, 2005]. Here we use BTD only to investigate the diurnal cycle in a consistent way. BTD is adopted as a proxy for dust and cirrus clouds as in work by *Chaboureau and Pinty* [2006]. It is the first time that such a technique is used to evaluate a time series of dust and cirrus cover forecasts against MSG observations.

[5] The BTD technique is applied to daily forecasts performed during the 2 week African Monsoon Multidisciplinary Analyses (AMMA) forecasting exercise using 3-hourly MSG observations. The forecasting exercise allows to test a prognostic dust scheme and its impact on the forecasts. Section 2 presents the model and the satellite observations. Section 3 provides an analysis of the dust and cirrus cover and discusses their diurnal cycle, in particular over West Sahara. Section 4 concludes the study.

2. Model and Satellite Observations

[6] The Meso-NH model [*Lafore et al.*, 1998] is adopted as a non-hydrostatic regional model. Vertical grid spacing in the free troposphere is set to 600 m, with horizontal grid spacing of 30 km. The model includes a 1.5-order turbulence scheme, an interactive radiation, and a prognostic microphysical scheme for 5 precipitating and non-precipitating liquid and solid water categories [*Pinty and Jabouille*, 1998] with a modified ice to snow autoconversion

[1]Laboratoire d'Aérologie, UPS/CNRS, Toulouse, France.
[2]Centre National de Recherches Mtorologiques/Centre National de Recherches Meteorologiques, Météo-France, Toulouse, France.

Copyright 2007 by the American Geophysical Union.
0094-8276/07/2006GL027771

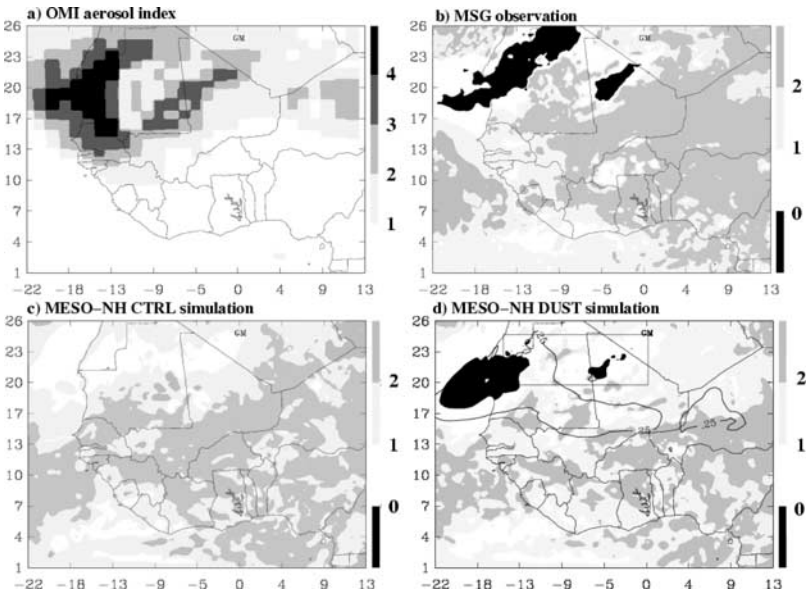

Figure 1. (a) OMI aerosol index and BTD (K) between 10.8 and 12 μm bands at 12 UTC 26 August 2005 obtained from (b) the MSG observations, (c) the CTRL and (d) DUST simulations. Black contours in Figure 1d are dust AOD larger than 0.25.

parameterization [*Chaboureau and Pinty*, 2006]. Deep and shallow convective transport and precipitation are parameterized following *Bechtold et al.* [2001]. Subgrid cloud cover and condensate content are parameterized as a function of the normalized saturation deficit by taking into account both turbulent and convective contributions [*Chaboureau and Bechtold*, 2005]. The dust scheme [*Grini et al.*, 2006] consists of the Dust Entrainment and Deposition (DEAD) model [*Zender et al.*, 2003] that calculates dust fluxes from wind friction coupled with the ORILAM model that follows the evolution of two moments of three modes (fine, accumulation, coarse) of lognormal aerosol distribution [*Tulet et al.*, 2005]. The distribution parameters are taken from the Saharan aerosol study of *Alfaro et al.* [1998].

[7] The dust impact on weather forecasts is tested through a regional climatological study of cloud systems observed during the AMMA dry run. From 22 August to 2 September 2005, a total of 12 daily 48-hour (CTRL) forecasts were run over a domain of 3840 km $\times$ 2880 km covering West Africa. The individual forecasts were initialized with 12-h ECMWF forecasts based on the 12 UTC ECMWF analyses. The initial and boundary conditions of the numerical experiments are provided for the horizontal wind, the temperature, and the water vapor. Clouds are not initialized, so the mixing ratios of the liquid and ice water species build up during the course of the simulations. The control (CTRL) runs were performed using aerosol climatology whereas additional simulations (DUST) were run using the dust scheme.

[8] Brightness temperatures (BT) corresponding to the MSG observations are computed using the Radiative Transfer for Tiros Operational Vertical Sounder (RTTOV) code version 8.7 [*Saunders et al.*, 2005]. The surface emissivity is given by the Moderate Resolution Imaging Spectroradiometer (MODIS) MYD11C3 product. Hexagonal columns are assumed with radiative properties taken from [*Baran and Francis*, 2004] and with an effective dimension diagnosed from the ice water content [*McFarquhar et al.*, 2003]. RTTOV has been adapted to take into account the aerosol extinction effect using the mineral transported model from the OPAC database [*Hess et al.*, 1998]. As for clouds, we assume dust to be grey bodies.

3. Results

[9] The BTD technique is illustrated at 12 UTC 26 August 2005 (Figure 1). The aerosol index (AI) obtained from the Ozone Monitoring Instrument (OMI) [*Torres et al.*, 1998, 2002] shows the presence of aerosol over Mauritania and northern Mali. The areas with the largest AI values well match those with negative BTDs observed from MSG (Figure 1b). Here, the negative BTD is due to the larger absorption by dust at 10.8 μm than at 12 μm. The dust signal is reproduced for the DUST simulation only (Figure 1d). Note that the negative BTD area does not match the region with predicted aerosol optical depth (AOD) larger than 0.5 as the dust effect on BTD depends on its altitude [*Pierangelo et al.*, 2004]. The BTD signal can be also masked by the presence of cirrus cloud as revealed by observed BTD larger than 2 K. Such a signal is well reproduced by both the CTRL and DUST simulations, confirming a good capacity of the model to forecast the cirrus cover [*Chaboureau and Pinty*, 2006].

[10] The BTD technique applied to the MSG observations also allows us to monitor the dust and cirrus cover during the dry run (Figure 2). Observed BTD distribution over the domain presents a clear diurnal variation of its extreme values. The first percentile mostly varies between -1 and 0 K from midnight to midday. The midnight negative BTDs are partly associated with the decrease of the atmospheric water vapor that enhances the surface emissivity spectral contrast. (Surface emissivity over the Sahara is down to 3% less at 10.8 μm than at 12 μm according to MODIS retrievals.) As a result, this smooth

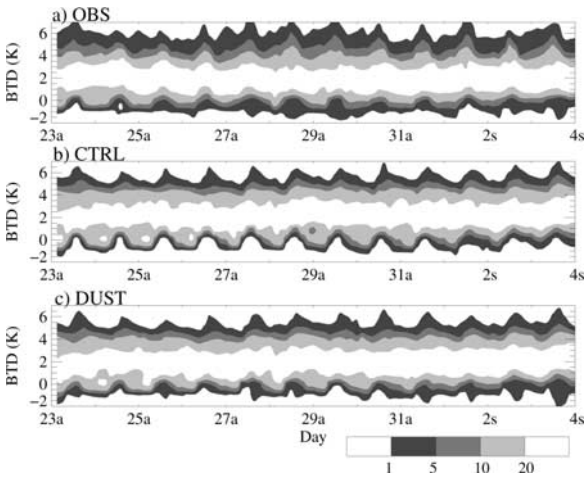

Figure 2. Time evolution of the BTD (K) distribution obtained from (a) the observations, and the 27–48 h forecasts of the (b) CTRL and (c) DUST simulations. The time axis is indicated by the day; a, August; s, September.

diurnal variation is captured by both the CTRL and DUST simulations. But some minimal values around −2 K observed at midnight are reproduced by the DUST simulation only, attributing this decrease in BTD to the presence of dust layers. On the other hand, the largest values of BTD are due to the diurnal variation of the cirrus cover, peaking around midday as also reported over northern Africa by *Tian et al.* [2004].

[11] Further statistics are obtained by averaging all the CTRL and DUST simulations over the 48-h forecast cycle and the observations over a diurnal cycle (Figure 3). The diurnal BTD variation due to the water vapor is filtered out by subtracting the diurnal negative BTD minimum obtained from the CTRL simulations (without dust) to the three data sets. As a result, the BTD in the CTRL simulations is always positive. In contrast, negative BTD are observed all day long with a peak at 15 UTC. This signal, due to the differential spectral dust absorption, is well reproduced by the DUST simulations. On the other part of the distributions, BTDs larger than 2–3 K are associated with the cirrus cover peaking at 12 UTC. The model reproduces correctly both the phase and the magnitude of the signal for both the CTRL and DUST simulations.

[12] The diurnal BTD variation due to the dust is further investigated by looking at the bi-diurnal cycle in the vertical section (Figure 4) obtained from the DUST simulations in a west Saharian area (15°W–0°, 20°–25°N) shown in Figure 1d. The variation of dust concentration with height follows the diurnal cycle of the convective PBL. A peak in dust is achieved at 18 UTC when the virtual potential temperature (θ_v) is almost constant between the ground and 4-km altitude. During night the nocturnal jet contributes to the dust mobilization that concentrates dust close to the surface while atmospheric dust particles can sediment with the collapse of the PBL. Next morning, the dust produced during nighttime is then entrained in the troposphere as soon as the solar heating develops a diurnal-mixed PBL. Note also the lowering of atmospheric water vapor during the night, a feature enhancing the dust detection. Such a diurnal cycle has also been reported from visibility observations [*N'Tchayi Mbourou et al.*, 1997] and from different

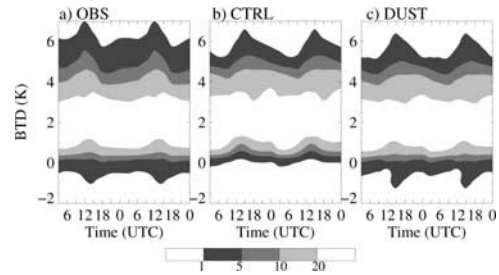

Figure 3. Bi-diurnal cycle of filtered BTD (K) distribution obtained from (a) the observations, and the 3–48 h forecasts with the (b) CTRL and (c) DUST simulations.

models using different dust source schemes [*Luo et al.*, 2004].

[13] Finally, the change in dust representation modifies the regional distribution of the AOD in the 48-h forecast with a large increase in the vicinity of Mauritania and a decrease elsewhere. The radiative forcing of the aerosol results in an increase of the equivalent potential temperature (θ_e) at the lowest model level over Mauritania (Figure 5a). Elsewhere over the Sahel, the decrease in θ_e is partly due to the low aerosol content in the first hours of the simulation. The increase in θ_e over tropical western Africa indicates that the aerosol forcing feeds back on convection. This is further shown using BT at 10.8 μm obtained from the 48-h forecasts and MSG observations (Figures 5b, 5c, and 5d). The change in stability makes the convection more intense around 10° N, giving simulated BTs closer to the observations. This reinforces the AEJ as shown by the wind at 650 hPa. This is similar to the change in the 5-day ECMWF forecasts [*Tompkins et al.*, 2005].

4. Conclusion

[14] A BTD technique is applied to MSG observations between the 10.8- and 12-μm bands in order to monitor the dust and cirrus cover during the AMMA dry run. When it is combined with the model-to-satellite approach, the BTD technique gives a specific constraint to the dust distribution. In particular, it highlights the diurnal cycle of dust over the Sahara. It also confirms the good capacity of the model to forecast cirrus cover at regional scales. Moreover, the model

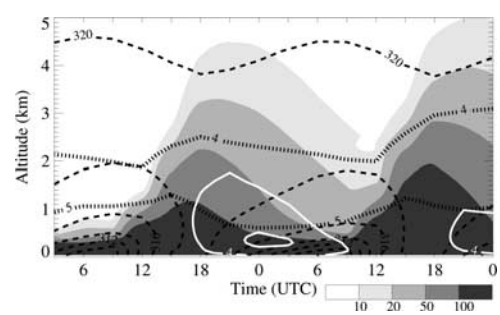

Figure 4. DUST evolution of the dust concentration (μg m^{-3}, shading), water vapor mixing ratio (thick dotted at 4 and 5 g kg^{-1},), θ_v (dashed, every 2 K), and wind speed (white contour at 4 and 6 m s^{-1},). Results are averaged over the Saharian box shown in Figure 1d from 3–48 hour forecasts.

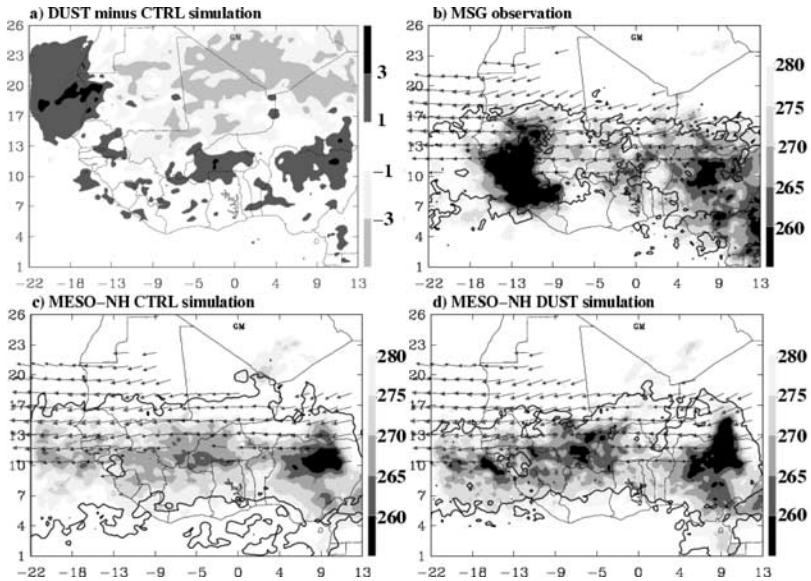

Figure 5. (a) Mean difference (DUST minus CTRL) in θ_e (K) at the lowest model level at 30 m from the 48-h forecasts. BT (K) at 10.8 μm (shading), BTD larger than 2 K (contours), and mean 650-hPa winds over 10 m s^{-1} (vectors) obtained from (b) the MSG observations and ECMWF analyses, and the 48-h (c) CTRL and (d) DUST forecasts. The maximum wind speed is 17 m s^{-1}.

result shows a positive impact on the simulated intensity of tropical deep convection and the associated wind fields, in particular the AEJ.

[15] The present technique is used to evaluate the cirrus and dust forecast of the model. One has to consider the combination of both cirrus and dust, thus their radiative properties, in order to utilize the BTD technique in its full potential. A combination of passive IR remote sensing technique and the space lidar CALIPSO has a high potential to provide an additional constraint on dust and cirrus modeling. Furthermore, the measurements taken during the AMMA experiment should help in documenting the mass distribution of dust. In near future, the next generation of operational models will operate with explicit bulk cloud schemes to be run at mesoscale with typical grid size of a few kilometers. A systematic evaluation with MSG observations, up to every 15 minutes, by the present approach would lead to substantial progress in dust and cirrus modeling. Finally, this approach also offers guidance to climate models for evaluating important model components such as the cirrus and dust schemes and their respective climate radiative impact.

[16] **Acknowledgments.** Computer resources were allocated by IDRIS. MSG observations and OMI retrievals have been obtained from SATMOS and the NASA/GSFC TOMS group, respectively.

References

Ackerman, S. A. (1997), Remote sensing aerosols using satellite infrared observations, *J. Geophys. Res.*, *102*(D14), 17,069–17,080.

Alfaro, S. C., A. Gaudichet, L. Gomes, and M. Maillé (1998), Mineral aerosol production by wind erosion: Aerosol particle sizes and binding energies, *Geophys. Res. Lett.*, *25*, 991–994.

Baran, A. J., and P. N. Francis (2004), On the radiative properties of cirrus cloud at solar and thermal wavelengths: A test of model consistency using high-resolution airbone radiance measurements, *Qu. J. R. Meteorol. Soc.*, *130*, 763–778.

Bechtold, P., E. Bazile, F. Guichard, P. Mascart, and E. Richard (2001), A mass flux convection scheme for regional and global models, *Q. J. R. Meteorol. Soc.*, *127*, 869–886.

Bechtold, P., J.-P. Chaboureau, A. Beljaars, A. K. Betts, M. Köhler, M. Miller, and J.-L. Redelsperger (2004), The simulation of the diurnal cycle of convective precipitation over land in a global model, *Q. J. R. Meteorol. Soc.*, *130*, 3119–3137.

Chaboureau, J.-P., and P. Bechtold (2005), Statistical representation of clouds in a regional model and the impact on the diurnal cycle of convection during Tropical Convection, Cirrus and Nitrogen Oxides (TROCCINOX), *J. Geophys. Res.*, *110*, D17103, doi:10.1029/2004JD005645.

Chaboureau, J.-P., and J.-P. Pinty (2006), Validation of a cirrus parameterization with Meteosat Second Generation observations, *Geophys. Res. Lett.*, *33*, L03815, doi:10.1029/2005GL024725.

Chaboureau, J.-P., J.-P. Cammas, P. Mascart, J.-P. Pinty, and J.-P. Lafore (2002), Mesoscale model cloud scheme assessment using satellite observations, *J. Geophys. Res.*, *107*(D16), 4301, doi:10.1029/2001JD000714.

Comstock, J. M., and C. Jakob (2004), Evaluation of tropical cirrus cloud properties and dynamical processes derived from ECMWF model output and ground-based measurements over Nauru island, *Geophys. Res. Lett.*, *31*, L10106, doi:10.1029/2004GL019539.

Grini, A., P. Tulet, and L. Gomes (2006), Dusty weather forecasts using the Meso-NH mesoscale atmospheric model, *J. Geophys. Res.*, *111*, D19205, doi:10.1029/2005JD007007.

Hess, M., K. Koepke, and I. Schult (1998), Optical properties of aerosols and clouds: The software package OPAC, *Bull. Am. Meteorol. Soc.*, *79*, 831–844.

Inoue, T. (1985), On the temperature and effective emissivity determination of semi-transparent cirrus clouds by bi-spectral measurements in the 10 μm window region, *J. Meteorol. Soc. Jpn.*, *63*, 88–98.

Lafore, J.-P., et al. (1998), The Meso–NH Atmospheric Simulation System. Part I: Adiabatic formulation and control simulations—Scientific objectives and experimental design, *Ann. Geophys.*, *16*, 90–109.

Luo, C., N. Mahowald, and C. Jones (2004), Temporal variability of dust mobilization and concentration in source regions, *J. Geophys. Res.*, *109*, D20202, doi:10.1029/2004JD004861.

McFarquhar, G. M., S. Iacobellis, and R. C. J. Somerville (2003), SCM simulations of tropical ice clouds using observationnaly based parameterizations of microphysics, *J. Clim.*, *16*, 1643–1664.

Morcrette, J.-J. (1991), Radiation and cloud radiative properties in the European Centre for Medium-Range Weather Forecasts forecasting system, *J. Geophys. Res.*, *96*(D5), 9121–9132.

N'Tchayi Mbourou, G., J. J. Bertrand, and S. E. Nicholson (1997), The diurnal and seasonal cycles of wind-borne dust over Africa north of the equator, *J. Appl. Meteorol.*, *36*, 868–882.

Pierangelo, C., A. Chédin, S. Heilliette, N. Jacquinet-Husson, and R. Armante (2004), Dust altitude and infrared optical depth from AIRS, *Atmos. Chem. Phys.*, *4*, 1813–1822.

Pinty, J.-P. and P. Jabouille (1998), A mixed-phase cloud parameterization for use in a mesoscale non-hydrostatic model: Simulations of a squall line

and of orographic precipitations, paper presented at Conference on Cloud Physics, Am. Meteorol. Soc., Everett, Wash.

Roskovensky, J. K., and K. N. Liou (2005), Differentiating airborne dust from cirrus clouds using MODIS data, *Geophys. Res. Lett.*, *32*, L12809, doi:10.1029/2005GL022798.

Saunders, R., M. Matricardi, P. Brunel, S. English, P. Bauer, U. O'Keeffe, P. Francis, and P. Rayer (2005), RTTOV-8 Science and validation report, NWP SAF report, 41 pp, Met Office, Exeter, U. K.

Sokolik, I. N. (2002), The spectral radiative signature of wind-blown mineral dust: Implications for remote sensing in the thermal IR region, *Geophys. Res. Lett.*, *29*(24), 2154, doi:10.1029/2002GL015910.

Tian, B., B. J. Soden, and X. Wu (2004), Diurnal cycle of convection, clouds, and water vapor in the tropical upper troposphere: Satellites versus a general circulation model, *J. Geophys. Res.*, *109*, D10101, doi:10.1029/2003JD004117.

Tompkins, A. M., C. Cardinali, J.-J. Morcrette, and M. Rodwell (2005), Influence of aerosol climatology on forecasts of the African Easterly Jet, *Geophys. Res. Lett.*, *32*, L10801, doi:10.1029/2004GL022189.

Torres, O., P. K. Bhartia, J. R. Herman, and Z. Ahmad (1998), Derivation of aerosol properties from satellite measurements of backscattered ultraviolet radiation: Theoretical basis, *J. Geophys. Res.*, *103*(D14), 17,099–17,110.

Torres, O., P. K. Bhartia, J. R. Herman, A. Sinyuk, and B. Holben (2002), A long term record of aerosol optical thickness from TOMS observations and comparison to AERONET measurements, *J. Atmos. Sci.*, *59*, 398–413.

Tulet, P., V. Crassier, F. Cousin, K. Suhre, and R. Rosset (2005), ORILAM, a three-moment lognormal aerosol scheme for mesoscale atmospheric model: Online coupling into the Meso-NH-C model and validation on the Escompte campaign, *J. Geophys. Res.*, *110*, D18201, doi:10.1029/2004JD005716.

Yoshioka, M., N. Mahowald, J.-L. Dufresne, and C. Luo (2005), Simulation of absorbing aerosol indices for African dust, *J. Geophys. Res.*, *110*, D18S17, doi:10.1029/2004JD005276.

Zender, C. S., H. Bian, and D. Newman (2003), Mineral Dust Entrainment and Deposition (DEAD) model: Description and 1990s dust climatology, *J. Geophys. Res.*, *108*(D14), 4416, doi:10.1029/2002JD002775.

J.-P. Chaboureau and C. Mari, Laboratoire d'Aérologie, OMP, 14 av. Belin, F-31400 Toulouse, France. (jean-pierre.chaboureau@aero.obs-mip.fr)

P. Tulet, Centre National de Recherches Mtorologiques/Centre National de Recherches Meteorologiques, Météo-France, Toulouse, France.